12th International Conference on Fracture Mechanics of Concrete and Concrete Structures
FraMCoS-12
B.L.A. Pichler, Ch. Hellmich, P. Preinstorfer (Eds)

https://doi.org/10.21012/FC12.1260
MS18-2:3

INTERFACE MODELLING IN NONLINEAR FINITE ELEMENT ANALYSIS OF PRESTRESSED GIRDER WITH A CONTINUOUS CAST-IN-SITU DECK SLAB

M. PETRANGELI[*], D. ADDESSI[*], N. KOSTENSE[†] AND J. G. ROTS [†]

[*]Sapienza University of Rome, Department of Structural Engineering
Via Eudossiana 18, 00184 Roma, Italia
e-mails: petrangeli.1876546@studenti.uniroma1.it, daniela.addessi@uniroma1.it, www.uniroma1.it

[†] Delft University of Technology, Faculty of Civil Engineering and Geosciences
Stevinweg 1, 2628 CN Delft, Netherland

Key words: Prestressed concrete beam, smeared crack model, concrete-to-concrete interface, finite element analysis

Abstract: With the advancement of computational techniques, numerous nonlinear constitutive laws have become available in finite element analysis software. While these models are well-suited to analyze plain and simple reinforced concrete structures, their applicability to prestressed structures, which constitute a significant portion of concrete constructions, requires validation. This study presents a finite element (FE) model composing a prestressed composite concrete girder, incorporating nonlinear stress-strain laws for the concrete, reinforcement steel and prestressing steel, as well as the concrete-to-concrete interfaces between prefabricated girder and cast-in-situ top-slab. To accurately capture the fracture process of the concrete, the total strain crack model is employed while the potential failure of the interface between the prefabricated girder and cast-in-situ top slab is modelled with two-dimensional line interface elements. The numerical model is validated using experimental results from precast continuous concrete inverted T-beams provided by TU Delft. A parametric study is subsequently conducted to assess the sensitivity of the numerical results to key assumptions in the nonlinear FE model. Specifically, the influence of adopting either a rotating or fixed crack model under high axial load is analyzed. Additionally, the effects of the shear retention factor and mesh size on the numerical response are investigated. While the numerically evaluated global load-displacement behavior shows good agreement with experimental results, it exhibits a sensitivity to the chosen mesh size and the specific smeared crack formulation. The findings also highlight the importance of considering the specific material properties and interface behavior in the modeling process to ensure reliable predictions of structural performance.

1 INTRODUCTION

Over the past 50 years, research focused on predicting the fracture process in concrete has gained popularity due to its added value in practical applications. These efforts have led to the development of several constitutive models for describing quasi-brittle behaviour of materials such as concrete under complex loading conditions. In numerical simulations of reinforced concrete structures using the Finite Element (FE) Method, two main approaches have been established and successfully employed to describe cracking phenomena: the discrete and smeared concepts. In the discrete crack concept, a crack is introduced as a geometric entity, enforcing the crack to propagate along the boundaries of

the continuum elements. Due to the predefined location of the cracks this procedure tends to introduce mesh bias [1-2]. In 1968, Rashid's introduction of the smeared crack concept proved to be a more advantageous alternative due to its computational efficiency and versatility. In contrast to the discrete approach, the smeared crack model treats a cracked material as a continuum, preserving the original finite element mesh topology. This is achieved by describing the material response through stress-strain constitutive relationships. Smeared crack models are roughly classified into three categories: fixed, multi-directional, and rotating approaches. The fixed approach maintains the crack orientation once initiated, while the rotating approach imposes the crack orientation to align with the principal strain axes throughout the computational process [3-4]. In the literature, the fixed crack approach is commonly used for reinforced concrete beams without shear reinforcement, where it accurately predicts flexural shear failures when combined with a damage-based shear retention function. The rotating crack approach, on the other hand, is preferred for beams with shear reinforcement, as it allows for the correct rotation of compressive struts and proper shear force distribution over stirrups. Although the rotating crack model has its advantages over the fixed format, it can suffer from over-rotating cracks, potentially leading to unrealistic behaviour [5-6]. For prestressed concrete beams, the choice between the two models still requires validation to determine the most suitable approach.

Another critical aspect of some special type of prestressed concrete beams is the interface between concrete layers cast at different times. Such interfaces are formed either during the initial construction or as a result of subsequent construction activities, such as repairs, retrofitting, or the connection of precast elements to cast-in-place concrete. This connection between various concrete layers can potentially entail a weak point. Modern construction techniques often incorporate cast-in-place concrete with precast components. Understanding the shear transfer mechanisms at concrete-to-concrete interfaces is crucial in the performance of concrete structures [7-8]. The physical and chemical processes governing the shear resistance at these interfaces include adhesion, aggregate interlock, friction, dowel action and rebar kinking. The various shear mechanisms do not act independently but interact with each other, affecting the overall shear resistance. As shear slip increases, the contribution of adhesive bonding progressively decreases. To account for the effect of adhesive bonding on the ultimate load, it requires the slip at failure to remain very small, typically no larger than about 0.05 mm [9]. The actual contribution of each mechanism depends on factors such as interface roughness, quality of bond, and the amount of reinforcement crossing the interface. Joints with increased reinforcement and rougher surfaces exhibit more ductile behavior, failing at larger slips compared to joints with less reinforcement or smoother surfaces. In interfaces with high roughness and substantial reinforcement, significant shear resistance remains even after significant slip, due to the combined effects of friction, dowel action, and kinking of the rebar [9-10]. To ensure proper integration and load transfer, the interface between the concrete layers needs to be carefully designed and assessed.

This study presents the nonlinear numerical analysis of prestressed concrete beams, with a particular focus on the interfaces between concrete layers cast at different times. The analysis relies on the results of a recent experimental campaign conducted at TU Delft on precast continuous concrete inverted T-beams. These experiments are unique and complex, making the validation of the numerical modelling approach challenging. Furthermore, it is of great interest to investigate the sensitivity of the numerical results to key modelling assumptions and input parameters.

The performance of the smeared crack approach in combination with a discrete interface that aims to capture the failure of the connection remains underexplored in the literature. To model the prestressed composite girder including construction stages, the FE

code DIANA was adopted. It is however noted that the assumptions and considerations on the modelling approach are general and not restricted by the specific software used. The Total Strain Crack (TSC) model is used to simulate concrete behavior according to the smeared crack approach. This model, developed based on the proposal by Feenstra and Rots [11], employs a single stress-strain relationship to represent both the tensile and compressive behavior of the material. This approach enables an explicit representation of the material's intrinsic nonlinearities [12-13]. An important aspect of the developed FE model concerns the incorporation of the interface between concrete layers cast at different times. In this study, a relatively simple model is employed to represent the concrete-to-concrete interface, adopting a nonlinear elastic model approach. The numerical results obtained from the nonlinear FE analyses provide insights into the performance of the considered smeared crack formats adopted to model these types of prestressed beams. Additionally, the results reveal the sensitivities of the analysis with respect to the adopted mesh size and shear retention factor.

2 EXPERIMENTAL RESULTS

The experimental campaign on a full-scale precast concrete inverted T-beam made continuous, provided by TU Delft [14], served as a reference for the numerical simulations presented in the following section. As part of a study program on the safety assessment of precast concrete bridges now in use, funded by the Dutch Ministry of Infrastructure and Water Management (Rijkswaterstaat), the specimen under investigation is the composite concrete girder in Fig. 1. The specimen has been part of a blind prediction contest organized in an effort to better understand the structural behavior, validate and enhance modeling methods for concrete structures without pre-knowledge of the experimental results. The specimen consists of two precast concrete beams, with a main span beam length of 11.25 m and a cantilever length of 3.50 m, separately fabricated at a precast plant. Subsequently, these beams are connected and made continuous using a cast-in-place top-layer and cross beam, ensuring structural continuity. At the interface between the precast beams and the cast-in-place top-slab, hairpin reinforcement, in the form of inverted U-shaped bars is present. The main girder has a straight strands layout with individual strand loaded till F_p = 79.0 kN. The shorter cantilever beam has a larger amount of prestress and shear reinforcement in the web to prevent premature (shear) failure. Each strand of the cantilever beam was pretensioned with a prestressing force of F_p = 118.5 kN.

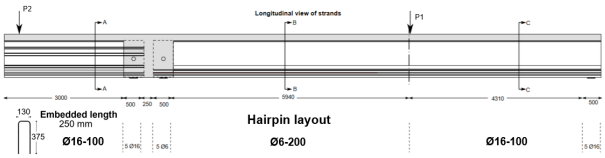

Figure 1: Precast continuous concrete inverted T beam.

Two hydraulic jacks, denoted as P1 and P2, are utilized to apply loads to the specimens. Jack P1 operates under displacement control loading at a constant rate of 0.02 mm/s, while jack P2 is force controlled, with its magnitude based on real-time readings from jack P1. A constant loading ratio of P1:P2 = 1:0.63 is maintained until either shear failure or yielding of the flexural reinforcement in the topping at the intermediate support region occurs. The experimental results of the test specimen are contained in Fig. 2, depicting the applied loads P_1 and P_2 versus the vertical displacement measured at the bottom of the beam, in line with the loading jacks respectively.

The load-deflection curves show two peak values of the ultimate load. After the first peak load has been reached, a significant drop is observed due to loss of composite action of the beam, initiated by cracking of the interface between the top slab and the beam. From a structural perspective, the structural integrity is compromised. Nevertheless, the experiment is still capable of proceeding with increasing load values. The beam eventually fails due to crushing in the upper part of the web under P1, which is the second peak load. In addition to

the load-displacement curves, the crack pattern of the specimen at the experimentally determined failure load is provided. The post-peak crack pattern is shown in picture in Fig. 3, taken from the intermediate support zone where the governing failure crack is observed.

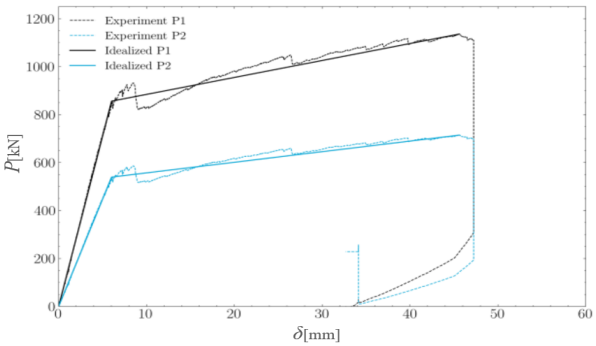

Figure 2: Idealized and experimental load-deflection curve for the specimen taken from [14].

Figure 3: Crack pattern at the end of the experimental test taken from [14]

3 FINITE ELEMENT MODELLING

To accurately capture the complex structural behavior of composite girders, including all relevant nonlinearities, the analyses in this study are conducted using DIANA FEA 10.7 software. The analysis settings, including load increments, iterative procedures, and convergence criteria, were meticulously configured in accordance with the guidelines established by the Dutch Ministry of Infrastructure and Water Management [15]. A two-dimensional modelling approach was adopted utilizing quadrilateral plane stress elements to model the concrete beam. More specifically, the CQ16M element is an 8-node quadrilateral isoparametric element that employs quadratic interpolation for the displacement fields and adopts a Gauss integration rule [12]. To model the interfaces, 3-node line interface elements are placed between the loading plates, as well as between the supporting plates (representing the bearings) and the beam. The CL12I element was used with quadratic interpolation for the relative displacement fields and a default 3-point Newton-Cotes integration scheme is adopted [12]. Embedded reinforcements were employed to model the prestressing strands and reinforcement bars, among longitudinal reinforcement, stirrups, hairpins, etc. The reinforcements are incorporated into structural elements and do not possess their own degrees of freedom; instead, their strains are derived from the displacement field of the mother elements, assuming a perfect bond between reinforcement and surrounding material [12].

The concrete is modelled using the Total Strain Crack (TSC) model. During the loading path, the concrete experiences both tensile and compressive stresses, potentially leading to cracking and crushing of the material. Various tensile and compressive constitutive laws can be adopted. Herein, the nonlinear softening curve according to Hordijk [17] was adopted in tension. A parabolic curve is selected for compressive behavior based on Feenstra's description of fracture energy [18]. The stress-strain relations are illustrated in Figure 4. By adopting strain-softening behavior, the fracture tends to localize in narrow bands, leading to mesh-dependency of the numerical solution [19-20]. These phenomena can be mitigated by introducing an internal characteristic length, called crack bandwidth (h), providing finite and non-zero energy dissipation during failure [17-21]. The specific fracture energy g_f is now obtained by dividing the fracture energy G_f with the crack bandwidth, where the subscript '$_f$' is equal to '$_t$' or '$_c$' for tensile and compressive law, respectively. In this study, Govindjee's projection method is used to compute the crack bandwidth, taking into account the crack orientation, element size and element aspect ratio. Only the characteristic element length h and the fracture energy G_c control the softening portion of the curve. The fracture energy in compression, G_c, was taken to be approximately 250 times G_t, in accordance with the formula provided in [15]. Considering that the compressive strength of cracked concrete is decreased by significant tensile strains perpendicular to the major

compressive direction, the reduction factor due to lateral cracking is introduced according to the model by Vecchio and Collins in [22]. To account for the shear stiffness reduction after cracking in the fixed crack format, a damage-based and a constant shear retention function of 0.01 were used. Finally, an orthotropic formulation for Poisson ratios is utilized to take into consideration that the Poisson effect disappears when the material is cracked and stretching in the crack's direction does not cause contraction in the perpendicular directions.

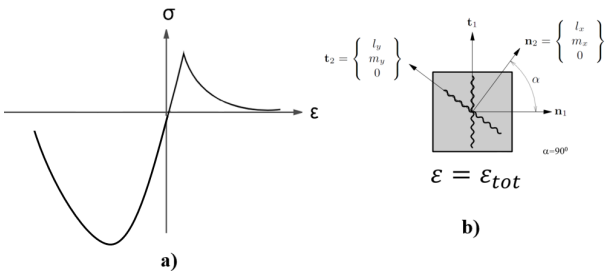

Figure 4: Example of Total strain crack model taken from [12]: uni-axial stress-strain law (a), crack rotation in the intrinsic reference system (b).

As for the material model for the interfaces, in this study a distinction is made between a strong and a weak interface between the prefabricated girder and cast-in-situ top slab. In the "*strong interface*" is assumed that the resistance is dominated by the combination of friction, dowel action, and aggregate interlocking mechanisms. Conversely in the *"weak interface"* the peak shear resistance primarily relies on the adhesive strength. As the adopted model does not allow for softening like behavior, only the post-peak shear resistance is considered. The simplified adopted interface constitutive laws are shown in Figure 5. For both types of interfaces, the shear strength was calculated using the formula proposed by Liu, Bu et al. in [16]. In the "*strong interface*" adhesion provides a shear strength of approximately 2-3 MPa at a slip value of 0.05 mm [9]. Beyond this point, the shear strength continues to increase due to additional resisting mechanisms, such as friction, which are significant because of the high reinforcement. In the *"weak interface"* the contribution of additional resisting mechanisms is smaller than that of adhesion. In this case, adhesion is disregarded in the model, and the shear strength at 0.05 mm slip does not reach the 2–3 MPa value expected from adhesion alone. Instead, it levels off at a lower value determined solely by the other shear resisting mechanisms. The drop-off in shear capacity was deliberately excluded from this constitutive model.

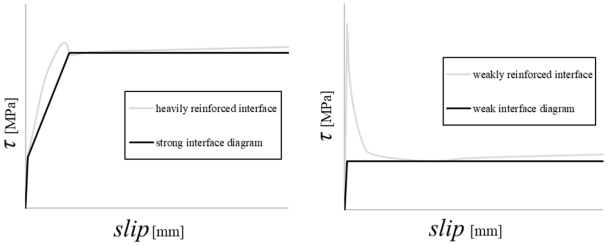

Figure 5: Shear traction vs slip constitutive law.

The bearings and loading plates are assumed to behave as isotropic and linear elastic materials. Since loading jacks have certain dimensions, applying the load as a concentrated force on the girder does not accurately reflect reality. Therefore, to distribute the load more evenly, the stiffness of the loading plates is taken into account and the adjacent stiffness of the structural interface was increased by a factor of 100 in the normal direction. The material reinforcement bars, including the prestress strands, were modelled adopting the Von Mises plastic formulation with isotropic strain hardening.

With the element types, material models, loading, and boundary conditions defined, a number of nonlinear structural analyses were performed. The simulations were conducted using a phased analysis approach which reflects the construction stages of the composite beam. The experimental load was applied using displacement-controlled loading with a prescribed deformation increment of 0.1 mm, while the dead loads from the previous phases were applied in a single step during phase initialization. A regular Newton-Raphson iteration method was used to solve the nonlinear problem in each loading step. Energy and force norms were selected with convergence tolerances equal to 0.001 and 0.01, respectively. In the sensitivity analysis,

various meshes with element sizes of 100 mm, 50 mm, and 25 mm were used, equal to approximately 1/10, 1/20, and 1/40 of the beam height, were adopted.

4 NUMERICAL RESULTS VERSUS EXPERIMENTAL OUTCOMES

The numerical global capacity curves obtained using the rotating crack approach for different mesh sizes are shown in Fig. 6. The curves exhibit the same initial elastic stiffness up to a displacement value of approximately 5 mm. Results with FE sizes of 100 mm and 200 mm show the end of the linear elastic regime of the girder at slightly lower displacements and load values as compared to finer meshes with FE sizes of 50 mm and 25 mm. The curves with mesh sizes of H/20 and H/40 follow a similar trend with higher capacity values compared to coarse meshes, confirming the work of A. de Putter in [5]. The 25 mm size mesh has a 10% higher peak load compared to the coarser meshes. Regarding the ultimate displacement using the rotating crack model, the different meshes lead to values that vary by up to 20%. The maximum ductility is achieved with the 200 mm sized FE. Both the 25 mm and 100 mm meshes have an ultimate displacement of approximately 22 mm. With respect to the results of the fixed crack model, the same conclusions can be drawn and is illustrated in Figure 7. The results demonstrate how a finer element discretization leads to an increase in the capacity of the composite girder. At the same time, there is a 20% drop in global capacity at a relative displacement of about 17.5 mm, when using 25 mm and 50 mm of FE size. This drop is attributed to a lack of convergence, followed by a few converged steps, before the analysis becomes unstable. In the figures, this phenomenon is marked with a triangle, indicating the point where non-convergence occurs before the analysis eventually diverges. Due to the high instability of the analysis, the results obtained after these non-convergent steps cannot be considered reliable or valid. Comparing the different crack formats, Figure 8 shows a comparison between the fixed crack model with the results presented for a constant shear retention factor of 0.01 and with a damage-based shear retention factor, and the rotating crack model, by considering a 50 mm mesh size. When using a damage-based shear retention function the model fails to capture the beam nonlinear behavior; the initial elastic stage coinciding with the other models, whereafter it reaches an ultimate displacement of just 6 mm when divergence occurs. It is furthermore observed that the difference between the rotating and fixed crack approaches lies mainly in the ultimate displacement, with the fixed crack approach with a constant shear retention function resulting in about 15% lower ductility.

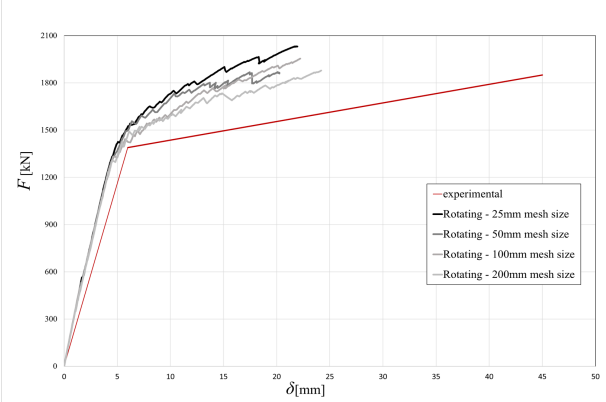

Figure 1: Load vs. displacement curves for rotating smeared crack approach for varying mesh size.

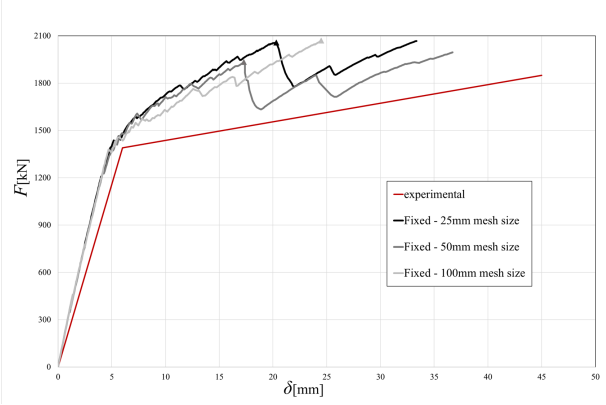

Figure 2: Load vs. displacement curves for fixed smeared crack approach for varying mesh size.

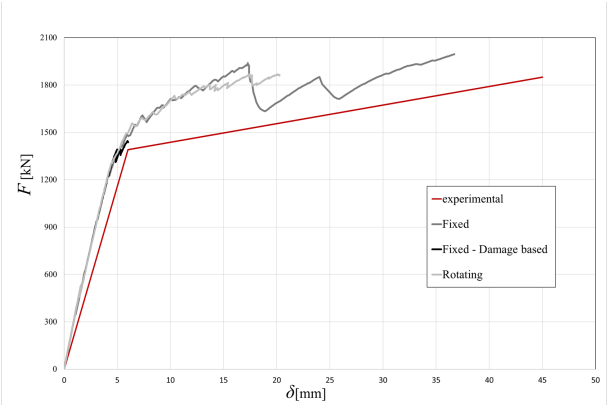

Figure 3: Load vs. displacement curves for 50 mm mesh size varying the used model.

In Figure 9 the crack plots are displayed for the rotating crack models with the variations in element sizes. It is observed that for the rotating crack model, a rather distinct vertical crack is formed for all meshes at intersection between the cross-beam and the prefabricated beam, most likely caused by lower tensile strength of the cross beam. Regarding the crack patter in the web near the intermediate support all models exhibit a very similar crack pattern characterized by the formation of a diagonal crack, propagating through the interface towards the midspan. Additionally, at the peak capacity, the formation of a bundle of cracks at the bottom of the beam under the load zone is observed, capturing the concrete crushing at the top. Referring to the results with a mesh size of 100 mm, it is noted that individual cracks cannot be distinguished, instead the crack are smeared out over the entire web. The same considerations are made by observing the crack pattern at peak load ofthe fixed crack model, as presented in Fig.10. The crack patterns displayed at the ultimate displacement for the rotating and fixed crack approach (with a constant shear retention) show consistent results, (Figure 11). A noticeable difference, however, is found in the magnitude of the crack size, which reaches significantly higher values for the rotating crack approach compared to the fixed crack approach. Nevertheless, a completely different scenario arises when a damage-based shear retention factor is adopted. Despite the formation of the vertical cracks at the intermediate support, no distinct diagonal crack is observed in the web. Instead, interface failure near the support is observed.

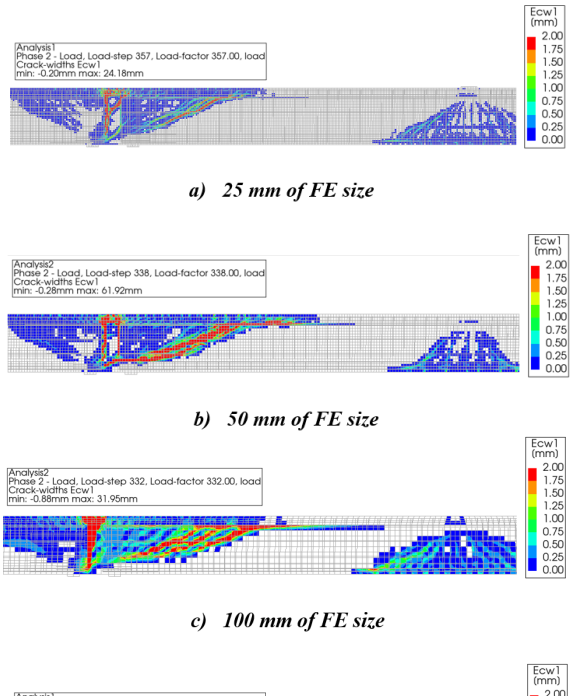

a) 25 mm of FE size

b) 50 mm of FE size

c) 100 mm of FE size

d) 200 mm of FE size

Figure 4: Numerical crack pattern at peak capacity for rotating smeared crack approach.

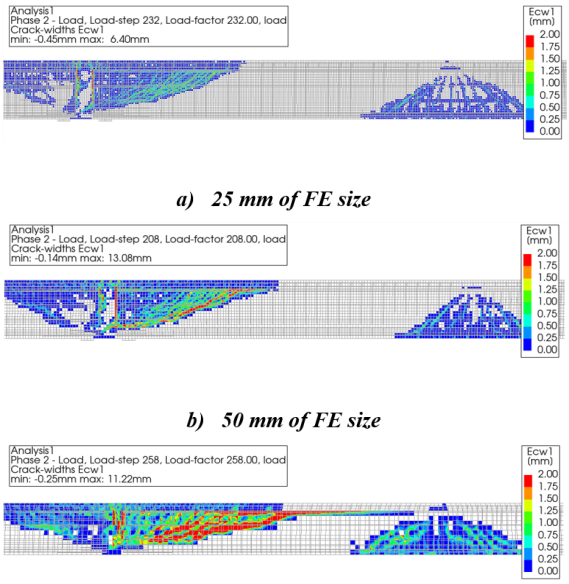

a) 25 mm of FE size

b) 50 mm of FE size

c) 100 mm of FE size

Figure 5: Numerical crack pattern at peak capacity for fixed smeared crack approach.

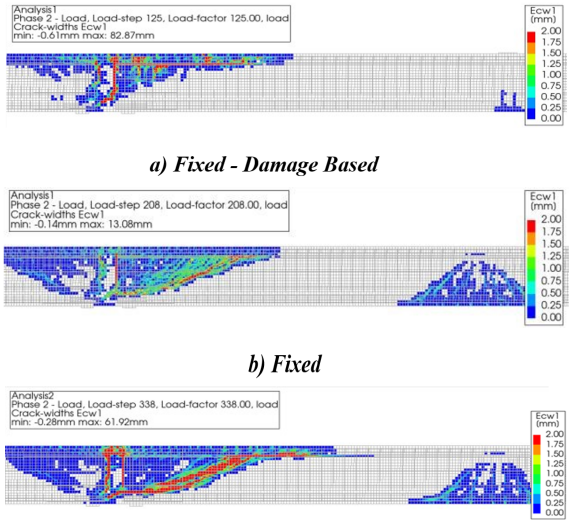

Figure 6: Numerical crack pattern at peak capacity for mesh with 50mm FE size.

5 CONCLUSIONS

In this study, multiple nonlinear FE analysis were conducted simulating a prefabricated concrete inverted T-beam made continuous, which was experimentally tested at TU Delft. A detailed FE model was developed by carefully selecting nonlinear material laws and associated mechanical parameters. Sensitivity analyses were performed to evaluate the influence of key modelling assumptions on the numerical results.

Taking the results in consideration, a trend with respect to mesh sizes is observed where a finer discretization leads to higher capacities and smoother load-displacement curves. With respect to the adopted crack format, the fixed crack approach, regardless of the shear retention factor (whether constant or damage-based), yielded lower capacity in terms of ultimate load and displacement compared to the rotating format. Moreover, the fixed crack approach with a damage-based shear retention factor showed significant stability issues and even divergence. On the other hand, the use of a constant shear retention factor led to results that are more sensitive to variations in the mesh size, suggesting them as less objective. Although all the crack formats give reasonable results, the rotating crack approach appears to be the most suitable choice for analyzing this specific prestressed beam. The analysis results demonstrate the ability of the numerical models to predict the development of the governing shear crack, which propagates through the interface and leads to failure of the specimen.

Finally, it is worth noting that the relatively simple nonlinear elastic model adopted for the concrete-to-concrete interface produced results that are in satisfactory agreement with the experimental outcomes. Such a modelling approach represents a good compromise between simplicity in formulation and accuracy in describing the global structural response.

6 ACKNOWLEDGEMENTS

This research was conducted by Marzio Petrangeli as part of his Master's Thesis exchange program. The presented work is part of ongoing research project at TU Delft funded by Rijkwaterstaat.

REFERENCES

[1] Rots, J.G., 1991. Smeared and discrete representations of localized fracture. *Int. J. Frac.* **51**:45-59.

[2] Borst, R., Remmers, J. J. C., Needleman, A., & Abellan, M. A., 2004. Discrete vs smeared crack models for concrete fracture: Bridging the gap. *International Journal for Numerical and Analytical Methods in Geomechanics*, 28(6), 583–607.

[3] Rots, J.G., 1988. Computational Modeling of Concrete Fracture. *Doctoral Dissertation, Delft University of Technology.*

[4] Petrangeli, M., & Ožbolt, J., 1996. Smeared Crack Approaches—Material Modeling. *Journal of Engineering Mechanics*, 122(6), 545-553.

[5] De Putter, A., 2020. Towards a uniform

and optimal approach for safe NLFEA of reinforced concrete beams. *Delft University of Technology*, April 24th.

[6] Kostense N., Yang Y., Hendriks M., & Rots J., 2023. A comparative study of implicit and explicit solution procedures for computational modeling of reinforced concrete structures. *Proceedings of the 2024 Fracture Mechanics of Concrete and Concrete Structures Conference (S. R. J. M. Chandra Kishen, A. Ramaswamy and R. Vidyasagar, eds.)*.

[7] Birkeland, P. W. and Birkeland, H. W., 1966. Connections in Precast Concrete Construction. *ACI Journal*, vol. 11, no. 42, pp. 345-368.

[8] Mattock, A. H., & Hawkins, N. M., 1972. Shear transfer in reinforced concrete – recent research. *Journal of the Precast/Prestressed Concrete Institute*, 17(2), 55-75.

[9] Randl, N., 2013. Design recommendations for interface shear transfer in fib Model Code 2010. *Structural Concrete*, 14(3), 230-241.

[10] Santos, P. M. D., & Júlio, E. N. B. S., 2012. A state-of-the-art review on shear-friction. *Engineering Structures*, 45, 435-448.

[11] Feenstra, P. H., Rots, J. G., Arnesen, J., Teigen, J., & Høiseth, K. 1998. A 3d constitutive model for concrete based on a co-rotational concept. *Conference on Computational Modelling of Concrete Structures*.

[12] Ferreira D., 2023. DIANA User's Manual -- Release 10.7.

[13] Wani, F. M., Khan, M. A., & Vemuri, J., 2022. 2D nonlinear finite element analysis of reinforced concrete beams using total strain crack model. *Materials Today: Proceedings*, 64, 1305-1313.

[14] Ibrahim, M.S., Kostense, N.W., Poliotti, M., Yang, Y., 2023, TU-Delft blind prediction contest on prestressed concrete beams made continuous, https://concrete-prediction-contest.tudelft.nl

[15] Hendriks M. A. N. and Roosen M. A., 2020. Guidelines for Nonlinear Finite Element Analysis of Concrete Structures. *Rijkswaterstaat Centre for Infrastructure*, *Utrecht*.

[16] Liu, J., Bu, Y., Chen, J., & Wang, Q., 2021. Contribution of Shear Reinforcements and Concrete to the Shear Capacity of Interfaces between Concretes Cast at Different Times. *KSCE Journal of Civil Engineering,* 25(6), 2065-2077.

[17] D. A. Hordijk, 1991. Local approach to fatigue of concrete. *PhD thesis, Delft University of Technology*.

[18] P. H. Feenstra, 1993. Computational Aspects of Biaxial Stress in Plain and Reinforced Concrete. *PhD thesis, Delft University of Technology.*

[19] Nocera, M., 2021. Micromechanical and macromechanical approaches for the analysis of periodic masonry structures. *University la Sapienza, Department of Structural and Geotechnical Engineering*.

[20] Addessi, D., 2000. Modelli di danno regolarizzati per materiali fragili. *University La Sapienza, Roma, Italy. Ph.D. thesis*.

[21] Pijaudier-Cabot, G., & Benallal, A., 1993. Strain localization and bifurcation in a nonlocal continuum. *International Journal of Solids and Structures*, 30(13), 1761-1775.

[22] Vecchio, F. J., & Collins, M. P., 1993. Compression response of cracked reinforced concrete. *J. Str. Eng., ASCE 119*, 12, 3590-3610.